Mitigating Voltage Collapse Problems in the Natal Region of South Africa

Franco de Villiers, *Eskom*
Marcos Donolo and Armando Guzmán, *Schweitzer Engineering Laboratories, Inc.*
Mani Venkatasubramanian, *Washington State University*

***Abstract*—The two main load centers in the Natal region of the Eskom power system are susceptible to voltage collapse. Voltage collapse problems near these load centers can be avoided by shedding load.**

This paper presents a real-time voltage stability system for voltage collapse mitigation and test results that validate the effectiveness of the system. This paper provides details on the implementation of the power system state determination functions, voltage stability indexes, load-shedding logic, and system operating time. The real-time voltage stability system gathers synchrophasor data to compute the power system state. The system uses the state and network data to obtain voltage collapse indexes. These indexes show how close the power system comes to voltage collapse and enable the real-time voltage stability system to effectively shed load and avoid voltage collapse.

I. Nomenclature

CLN	Customer load network
ILC	Incremental load cost
IRPC	Incremental reactive power cost
PFP	Power flow problem
PIM	Power import margin
PMU	Phasor measurement unit
QV	Reactive power to voltage
RTVSS	Real-time voltage stability system
SIPS	System integrity protection scheme
SVC	Static VAR compensator

II. Introduction

During peak load conditions, the Natal region of the Eskom power system in South Africa is susceptible to fast voltage collapse. To address this problem, we present an RTVSS. This system gathers synchrophasor data from the power system and identifies regions where voltage may collapse. Additionally, the RTVSS analyzes predefined contingencies to identify regions where voltage may collapse after the occurrence of each contingency.

In a previous paper [1], we proposed a system for real-time prediction and mitigation of the voltage collapse problem in the Natal region of South Africa. The previous paper presents results obtained offline to show the behavior of the voltage collapse prediction method.

III. Proposed System and Test Setup Overview

In this paper, we adapt the procedure proposed in [1] and implement the adapted procedure using a real-time vector processor [2] [3] and a generic computing engine. Fig. 1 identifies the main component of the RTVSS. The real-time vector processor provides time alignment and simplifies data sharing for automatic control, manual control, and visualization.

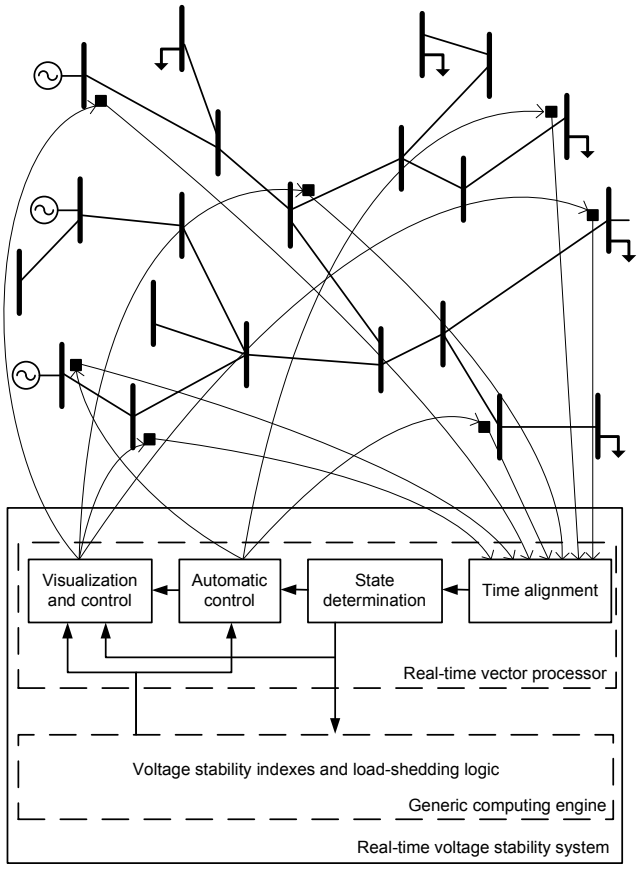

Fig. 1. Real-time voltage stability system

Fig. 2 shows the test setup that we use to test the proposed voltage stability system. The blocks of the test setup that run in real time are shaded gray. Using a detailed model of the Eskom power system ⓐ, a commercial dynamic simulation program ⓑ generates phasor data for selected buses ⓒ. Synchrophasor data from these buses are sent in separate IEEE C37.118 [4] streams ⓓ to the real-time vector processor. The real-time vector processor ⓔ time-aligns the synchrophasors, determines the state of the power system, and sends trip commands. The power system state includes the following data:

- Voltage phasors at every bus
- Branch status
- Transformer tap position
- Status of reactive power compensators

The power system state data are then sent to a computing engine ⓕ to determine voltage stability indexes and decide where and how much load to shed. The computing engine uses a reduced network model ⓖ to compute the voltage stability indexes. The voltage stability indexes, along with the trip signals, are sent back to the real-time vector processor, which displays these data and sends trip signals to relays or breakers to shed loads. In our test setup, we log the time of the trips ⓗ and the amounts of load to shed. We include these logged data in the dynamic simulation to obtain the closed-loop behavior of the system.

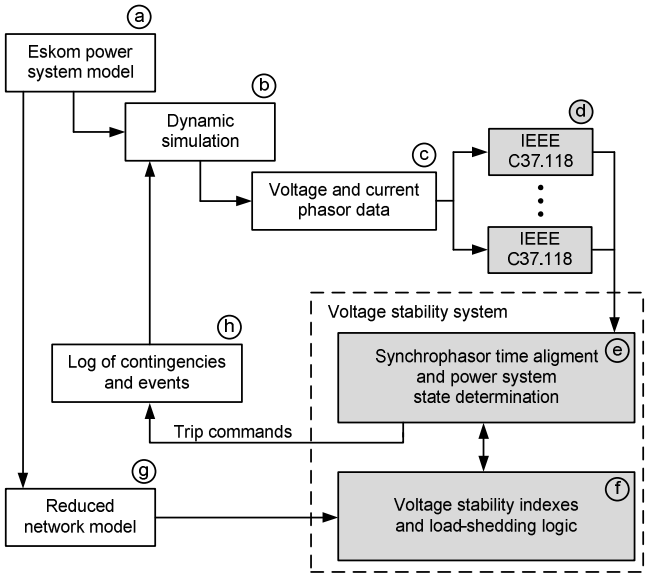

Fig. 2. Test setup to analyze the performance of the RTVSS

IV. Voltage Collapse at the Natal Region

A. Overview

The Natal network, shown in Fig. 3, is an integral part of the Eskom power system. Camden, Tutuka, Majuba, and Alpha are the buses that connect Natal to the rest of the Eskom network. Camden, Tutuka, and Majuba are large thermal plants. Drakensberg is a pumped storage station. SVCs are installed at Athene, Illovo, and Impala. The major load centers are the Empangeni CLN (2,150 MW) and Pinetown CLN (3,150 MW). The load in the remaining portion of the Natal network is 1,280 MW.

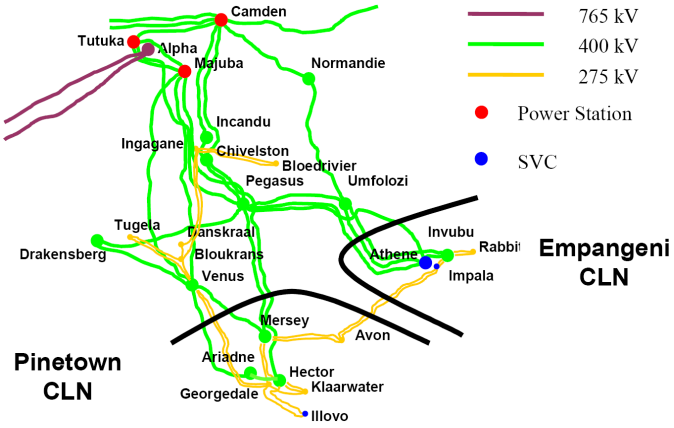

Fig. 3. Tie lines between the Natal network and the CLNs of Empangeni and Pinetown

Fig. 4 shows the load at the CLNs, the main transmission corridors and their active power flow, and the real power generation reserves of each generating station. The values shown in Fig. 4 correspond to peak summer load.

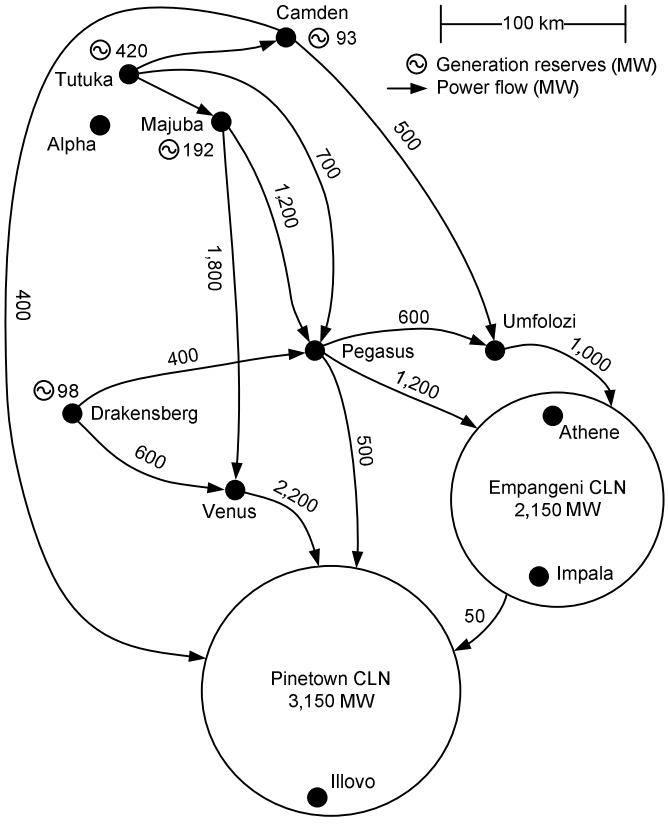

Fig. 4. Generation reserves and power flow in the Natal network, Pinetown CLN, and Empangeni CLN

B. Eskom Power System Model

Table I shows the number of elements in the different power system models that we use to evaluate the performance of the system. The second column of Table I shows the number of elements in the Eskom power system model used in the dynamic simulations. The third column shows the number of elements in the Natal subsystem. The fourth column shows the number of elements in the reduced model that we use to compute voltage stability indexes.

TABLE I
POWER SYSTEM ELEMENTS IN THE ESKOM POWER SYSTEM MODEL, THE NATAL SUBSYSTEM, AND THE REDUCED MODEL

Power System Elements	Eskom	Natal	Reduced
Buses	995	510	129
Transmission lines	1,098	694	138
Transformers	445	235	62
Loads	601	422	61
Machines	102	36	36
SVCs	4	3	3
Switched shunts	109	18	18

The choice of load models is critical in voltage stability studies. In this study, all loads are represented with models that keep P and Q constant for voltages greater than 0.7 per unit and reduce the output when the voltage is less than 0.7 per unit [5].

We modeled each SVC as a constant inductor in parallel with a synchronous condenser with a suitable output limit.

V. IMPLEMENTATION DETAILS

A. Time Alignment in the Real-Time Vector Processor

The time-alignment process in the real-time vector processor receives IEEE C37.118 synchrophasor data from the PMUs in the power system and creates a superpacket, where all the data have the same time stamp.

B. Direct State Determination

1) Branch Status

For voltage stability studies, it is important to determine the status of breakers and disconnects at each end of a transmission line because a long transmission line open at one end adds a large amount of reactive power to its connected end. If current measurements are available at one end of the transmission line, we use (1) to compute the expected current in case the remote end is open. If the measured current is close to the expected current, we conclude that the remote end is open. If the measured current is near zero, we conclude that the local end of the transmission line is open.

$$I_{exp} = V_s\left(\frac{Y}{2} + \frac{1}{Z + \frac{2}{Y}}\right) \quad (1)$$

2) Voltage Phasor Measurements

One inherent feature of traditional power system state estimators that we want to preserve in direct state measurement is their ability to handle redundant data sets. In this section, we show how to get this feature using direct measurements.

In our implementation, voltage phasors either are direct PMU measurements or are calculated using voltage synchrophasors, current synchrophasors, and network parameters. We use (2) to obtain the voltage phasor at the receiving end of a transmission line using phasor measurements from the sending end of the transmission line and the transmission line parameters. Fig. 5 specifies the variable names used in (2).

$$V_r = V_s - Z\left(I_s - \frac{YV_s}{2}\right) \quad (2)$$

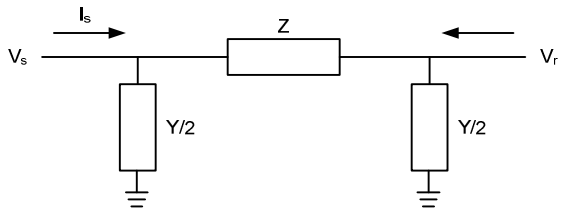

Fig. 5. Pi model of a transmission line to estimate voltage at the remote end

Our hypothesis for synchrophasor errors is that as long as all of the synchrophasor quality indicators are good, we assume the measurement is good. If redundant, direct, or calculated measurements are available, we take the median of all of the measurements as the reported measurement.

C. Computing Engine

Fig. 6 shows the tasks that the computing engine performs. Block A establishes communications links between the real-time vector processor and the computing engine. Block B uses the communications links to obtain power system data to put together the base power flow case. Block C calculates the voltage stability indexes and determines if load shedding is required. Block D calculates the voltage stability indexes for the contingency cases. The power flow engines in Blocks E and F provide the power flow solutions that the engine requires to compute the voltage stability indexes. Block G uses the communications links created in Block A to send the voltage stability indexes and trip commands to the real-time vector processor.

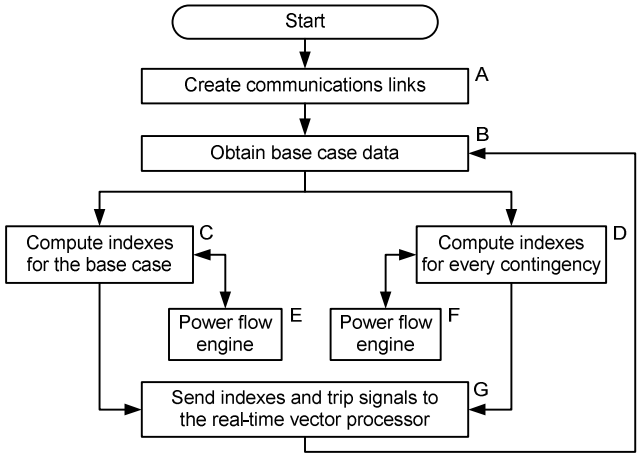

Fig. 6. Stability index calculation at the computing engine

1) Voltage Stability Indexes

a) QV Margin

For a given power system network under steady-state power flow conditions, the QV margin at a bus is defined according to (3) as the minimum addition of inductive load at the bus that causes voltage collapse.

$$\text{QV margin} = Q_{collapse} - Q_{base} \tag{3}$$

A procedure to obtain the QV margin at a bus involves solving PFPs by increasing inductive load at the bus until no power flow solution can be found [6] [7]. This procedure usually requires solving a large number of PFPs, which limits the use of the procedure for real-time applications. However, fast algorithms are available for calculating QV margins [8].

In general, a divergent power flow study is not equivalent to voltage collapse. A power flow run may diverge because the starting point is outside the region of attraction of the solution. In the RTVSS, we assume that divergent power flows are equivalent to voltage collapse because we start with a solved power flow case, obtained directly from the system, and we make incremental changes to the loads. This procedure minimizes the distance between the starting point and the solution.

b) Incremental Reactive Power Cost

The IRPC with respect to a given bus for a given loading condition is defined in (4).

$$IRPC_j = \frac{1}{\Delta Q_{bus_j}} \sum_{k=1}^{n} \Delta Q_{gen_k} \tag{4}$$

where ΔQ_{gen_k} is the change in the k-th generator reactive power output for a small change in the reactive power load at the bus, ΔQ_{bus_j}, and n is the number of reactive power sources. In this paper, $IRPC_j$ is computed by solving a PFP, adding 10 MVAR at Bus j, solving another PFP, and then computing all the differential quantities in the $IRPC_j$ ratio. When $IRPC_j$ equals 1, it means that consuming 1 extra MVAR at the bus requires generating 1 extra MVAR at reactive power sources. When $IRPC_j$ equals 2, consuming 1 extra MVAR at the bus requires generating 2 extra MVARs at the reactive power sources. The intuitive interpretation of $IRPC_j$ is how much reactive power needs to be provided by the reactive power sources to feed each additional MVAR at bus_j.

c) Incremental Load Cost and Load-Shedding Bus Selection

The ILC of a bus for a given loading condition is defined in (5).

$$ILC_j = \frac{1}{\Delta S_{bus_j}} \sum_{k=1}^{n} \Delta Q_{gen_k} \tag{5}$$

where ΔS_{bus_j} is a small change in the total load at Bus j. In this paper, ΔS_{bus_j} equals 10 MVA at 0.866 power factor. The intuitive interpretation of ILC is how much reactive power needs to be provided by the generators to feed each additional MVA at bus_j. ILC identifies critical loads that will relieve the largest amounts of reactive power from the reactive power sources when the MVA loads at those buses are reduced by load-shedding schemes.

d) Power Import Margin

The PIM of an area in a power system is the maximum amount of load that can be added in the area for which the system maintains stability. To compute PIM, it is important to accurately predict which generating stations pick up the additional load. For example, referring to Fig. 4, if we compute PIM for the Pinetown CLN assuming that the additional load is provided by generators at Drakensberg, we obtain a larger PIM value than we would obtain assuming that the additional load is provided by generators at Tutuka.

2) Amount of Load to Shed

The processing interval for the RTVSS is 1 second, which implies that the system can send several trip signals to avoid a voltage collapse event. Taking into account this processing interval, we decided to implement a fixed load-shedding step scheme in each interval.

3) Trip Decision

The trip decision may be based on either the QV margin or PIM exceeding a threshold. In our implementation, we used a threshold on the QV margin, because computing the QV margin does not require knowing the active power generation schedule. In a system where the active power generation schedule is known, PIM may be more meaningful than the QV margin.

D. SIPS Description

In addition to computing QV margins for the current power system state, the RTVSS proposed in this paper monitors the QV margins after simulated contingencies. When the QV margin falls below a user-defined threshold, the RTVSS arms the SIPS, which sheds load instantaneously after the contingency is identified. Fig. 7 shows the logic diagram of the SIPS.

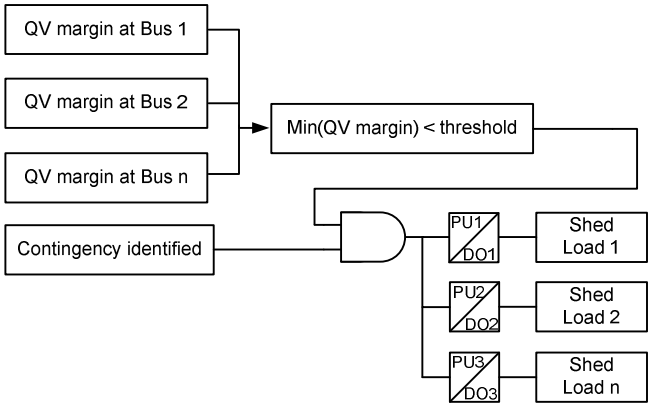

Fig. 7. SIPS to avoid sudden voltage collapse after a contingency

VI. RTVSS Performance Evaluation

A. Base Case

We base our test case on the Eskom power system configured for the system peak load conditions on July 5, 2007, at 6:30 p.m. In this configuration, the generators at Tutuka, Camden, Majuba, and Drakensberg are operating close to their active power full capacity, but plenty of reactive power is available at those buses. With the exception of the tie line between Venus and Mersey (see Fig. 3), all major transmission lines in the area are operating below or at about 50 percent of the maximum thermal capacity. To further stress the system, we remove the transmission line between Majuba and Pegasus. This transmission line carries 1,200 MW before removal. Removing this transmission line forces power flow through the bus at Venus and drains the reactive power reserves around Athene and Impala. The reactive power reserve in the SVC at Empangeni is 40 MVAR, which causes the QV margins to become critically low at the Empangeni CLN.

With our base power flow case, we start a dynamic simulation run, increasing the reactive power load at Athene and Impala to force a voltage collapse event. We increase the reactive power load at a rate of 8 MVAR/s on each bus. Fig. 8 shows the behavior of the voltages at Majuba, Umfolozi, and Athene.

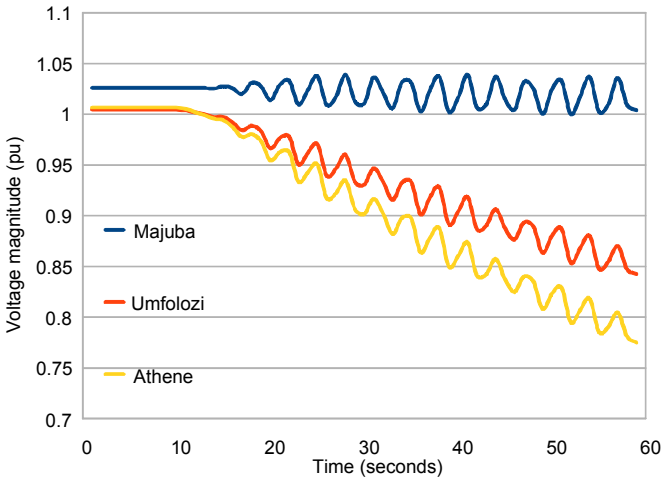

Fig. 8. Behavior of the voltage magnitudes for a constant increase in Q of 16 MVAR/s

Fig. 9 shows the behavior of the angle differences between Majuba and Umfolozi and between Majuba and Athene.

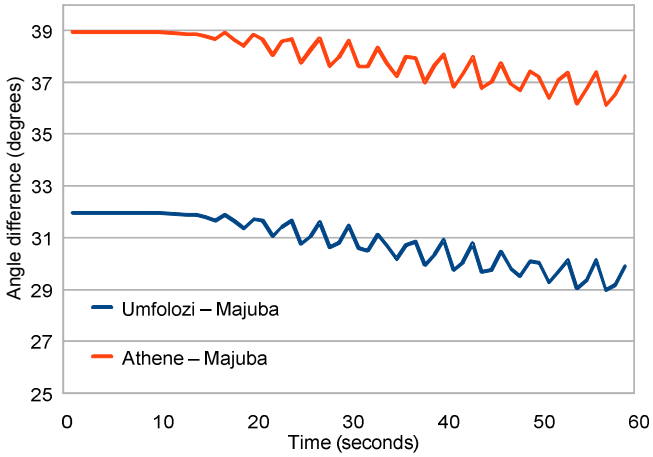

Fig. 9. Behavior of the voltage phasor angles for a constant increase in Q of 16 MVAR/s

Fig. 10 shows the QV margin obtained with the computing engine. Note that the computing engine updates the QV margin every second.

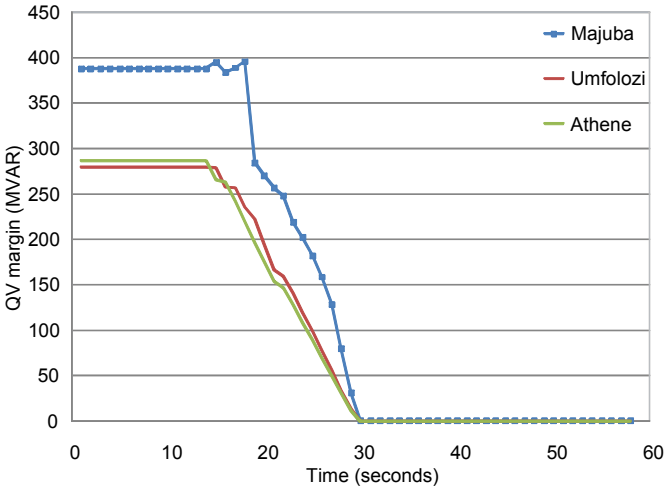

Fig. 10. Behavior of the QV margin for a constant increase in Q of 16 MVAR/s

Fig. 11 shows the IRPC obtained with the computing engine. Three stages can be identified in this figure. In the first stage, from 0 to 17 seconds, the IRPCs are less than 3. During this stage, the additional reactive power is mostly provided by local SVCs. During the second stage, between 17 and 21 seconds, the IRPCs at Athene and Umfolozi grow to 4, showing that the SVC at Athene is locked at its maximum. During the third stage, after 21 seconds, all local SVCs are locked at their maximum, and the IRPCs for the buses at Empangeni jump to values greater than 8.

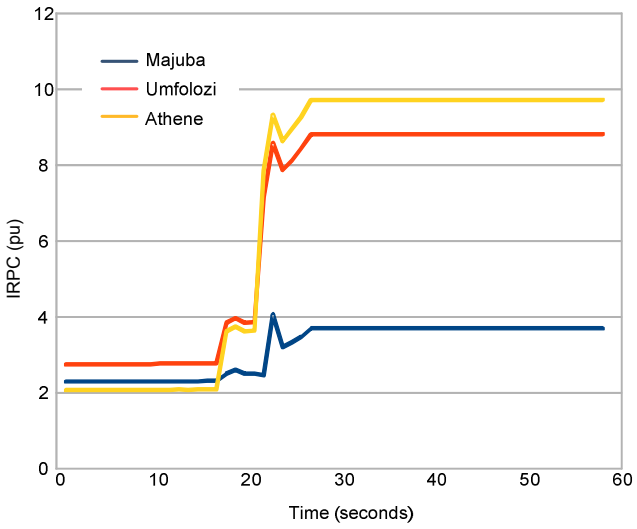

Fig. 11. Behavior of the IRPC for a constant increase in Q of 16 MVAR/s

B. *QV Margin-Based Load Shedding*

In this case, we set the RTVSS to shed load every time the QV margin at any bus falls below 100 MVAR.

Fig. 12 shows the behavior of the voltages at Majuba, Umfolozi, and Athene.

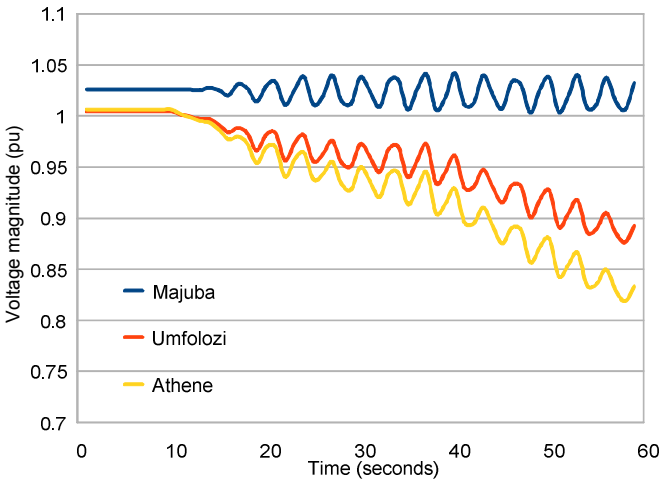

Fig. 12. Behavior of the voltage magnitudes for a constant increase in Q of 16 MVAR/s and automatic load shedding

Fig. 13 shows the behavior of the voltage phasor angles at Majuba, Umfolozi, and Athene, considering load shedding.

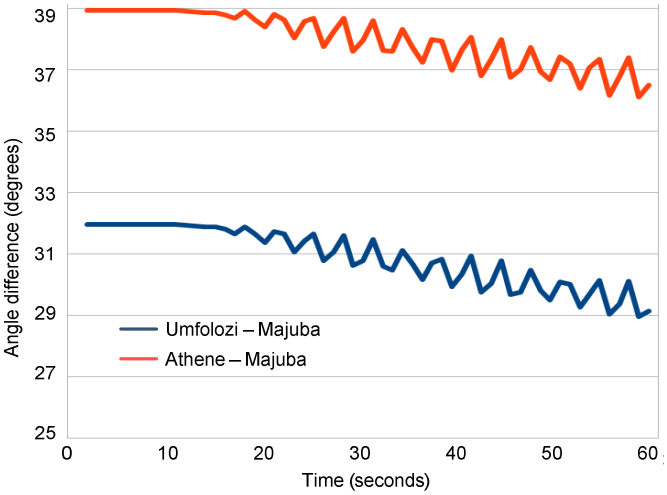

Fig. 13. Behavior of the voltage phasor angles for a constant increase in Q of 16 MVAR/s and automatic load shedding

Fig. 14 shows the QV margins. Every time the QV margin drops below 100 MVAR at one of the buses, the real-time vector processor sheds load in 50 MVA blocks to restore the QV margin. When the RTVSS runs out of load to shed at 40 seconds, the QV margin goes to zero MVAR, and the voltage magnitudes continue to fall, as shown in Fig. 12.

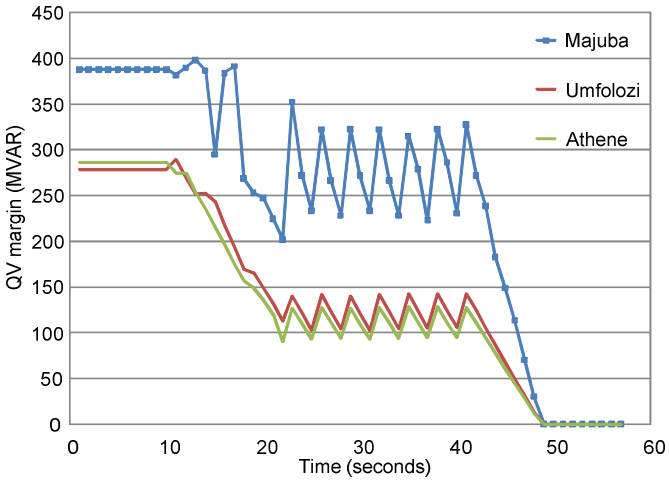

Fig. 14. Behavior of the QV margin for a constant increase in Q of 16 MVAR/s and automatic load shedding

When comparing Fig. 10 and Fig. 14, we observe that the RTVSS holds the QV margin above 100 MVAR for an additional 20 seconds. In our test case, the reactive load grows continually, driving the QV margin to zero at 50 seconds.

Fig. 15 shows the behavior of the IRPC considering load shedding. The three stages that we identified in Fig. 11 are present in Fig. 15, but in this case, the IRPC remains less than 4 for a longer period of time (16 seconds).

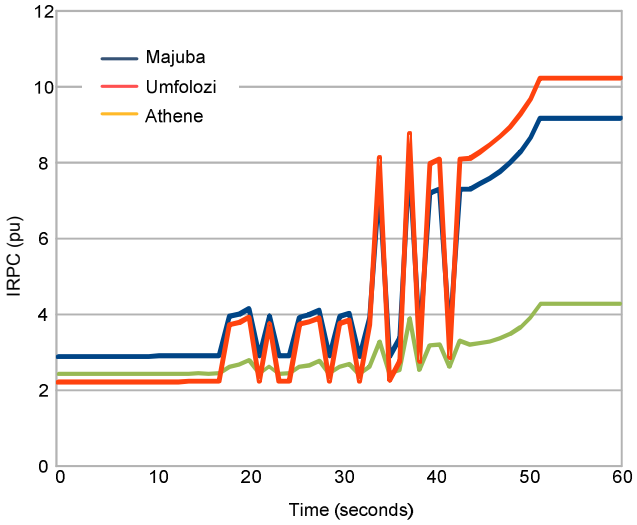

Fig. 15. Behavior of the IRPC for a constant increase in Q of 16 MVAR/s and automatic load shedding

C. SIPS Performance

In this contingency analysis, the RTVSS monitors the QV margins after a loss of the transmission line between Pegasus and Umfolozi. When the QV margin falls below 100 MVAR, the RTVSS arms the SIPS, which sheds load instantaneously after the contingency is identified.

Fig. 16 shows the QV margins at Athene. The top line is the QV margin computed using the power system state. The lower line is the QV margin computed simulating a contingency. In this case, the contingency drops the transmission line between Drakensberg and Pegasus. When the contingency QV margin falls below 100 MVAR, the RTVSS arms the SIPS. At 18 seconds, we disconnect the transmission line, and the SIPS drops load at Empangeni to avoid voltage collapse.

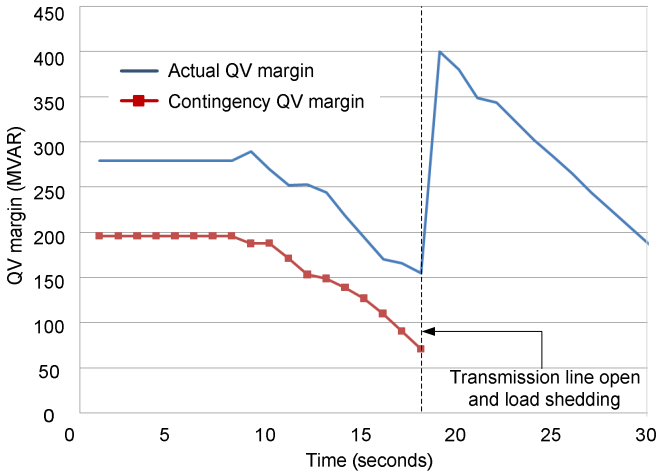

Fig. 16. SIPS restores the QV margin instantaneously after the contingency

Fig. 17 shows the voltage magnitudes for two cases. In one case (shown as solid lines), the transmission line is disconnected, and the SIPS sheds load. In the other case (shown as dashed lines), the transmission line is disconnected, but no load is shed. In the case with load shedding, the voltages at Umfolozi and Athene remain above 0.93 per unit for 10 seconds longer than in the case without load shedding.

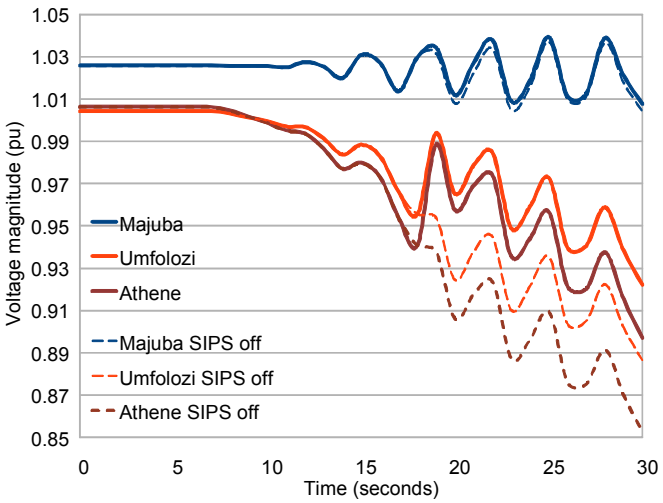

Fig. 17. Voltage magnitude recovers for 3 seconds after the SIPS sheds load

VII. Conclusion

This paper shows the implementation of an RTVSS that determines the state of the power system using synchrophasors, computes the QV margin at selected buses, and sheds load when the QV margin at a bus is less than a user-defined threshold. Additionally, the RTVSS evaluates predefined contingencies to arm a SIPS to shed load instantaneously to avoid sudden system collapse after a contingency. With a processing interval of 1 second, the RTVSS is able to shed load in a timely manner.

In our simulations of the Eskom power system model, the algorithm effectively identified proximity to voltage collapse and shed load accordingly to avoid system collapse.

The state determination functions and the test setup developed for the RTVSS can be applied independently to a wider range of problems. The test setup can be utilized to test other synchrophasor-based schemes, such as out-of-step and islanding detection schemes.

VIII. Acknowledgement

The authors thank Chuck Petras for helping to develop the communications links between the real-time vector processor and the computing engine and Francisco Velez for his contributions to the test setup.

IX. References

[1] M. Donolo, M. Venkatasubramanian, A. Guzmán, and F. de Villiers, "Monitoring and Mitigating the Voltage Collapse Problem in the Natal Network," proceedings of the IEEE PES Conference and Exposition, Seattle, WA, March 2009.

[2] E. O. Schweitzer, III, and D. Whitehead, "Real-Time Power System Control Using Synchrophasors," proceedings of the 34th Annual Western Protective Relay Conference, Spokane, WA, October 2007.

[3] E. O. Schweitzer, III, D. Whitehead, A. Guzmán, Y. Gong, and M. Donolo, "Advanced Real-Time Synchrophasor Applications," proceedings of the 35th Annual Western Protective Relay Conference, Spokane, WA, October 2008.

[4] *IEEE Standard for Synchrophasors for Power Systems,* IEEE Standard C37.118-2005. Available: http://standards.ieee.org.

[5] *PSS/E® 30.2.* Siemens Power Technologies International PSS/E Manual.

[6] C. W. Taylor, *Power System Voltage Stability*, McGraw-Hill, 1994.

[7] T. Van Cutsem and C. Vournas, *Voltage Stability of Electric Power Systems*, Springer, 1998.

[8] M. Venkatasubramanian, "Real-Time Voltage Security Assessment Using Synchrophasors," proceedings of the 34th Annual Western Protective Relay Conference, Spokane, WA, October 2007.

X. Biographies

Franco de Villiers received his BS in electrical and electronic engineering from the University of Potchefstroom (South Africa) in 1985, his honors degree in control theory from the University of Pretoria in 1992, and his masters from the University of the Witwatersrand (South Africa) in 2005. He has worked for Eskom since 1990 and has approximately 15 years of experience in load flow and network dynamics simulation and analysis.

Marcos Donolo received his BS in electrical engineering from Universidad Nacional de Rio Cuarto, Argentina, in 2000, and his masters degree in electrical engineering (2002), his masters degree in mathematics (2005), and his Ph.D in electrical engineering (2006) from the Virginia Polytechnic Institute and State University. Since 2006, he has been with Schweitzer Engineering Laboratories, Inc. in Pullman, Washington, where he is presently a research engineer. He is a member of IEEE.

Armando Guzmán received his BSEE with honors from Guadalajara Autonomous University (UAG), Mexico. He received a diploma in fiber-optics engineering from Monterrey Institute of Technology and Advanced Studies (ITESM), Mexico, and his MSEE from the University of Idaho, USA. He lectured at UAG and the University of Idaho on power system protection and power system stability. Since 1993, he has been with Schweitzer Engineering Laboratories, Inc. in Pullman, Washington, where he is presently research engineering manager. He holds several patents in power system protection and metering. He is a senior member of IEEE.

Vaithaianathan "Mani" Venkatasubramanian is presently a professor in electrical engineering at Washington State University, Pullman, Washington. His research interests include the stability analysis and control designs for large-scale power system models.